CHARACTERIZATION OF MICROGLIAL RESPONSE IN THE FEMALE 3xTgAD MODEL

Final Master Project

Author: Jorge Lucerón Morales

Supervisor: Francisco Ros Bernal

Master of Brain and Behavior Research

Faculty of Health Science

Universitat Jaume I

Castelló

July 31th, 2021

Abstract

Alzheimer's disease (AD) involves severe impairment of cognitive and executive functions and represents 60-70% of all cases of dementia. Neuropathologically, it is characterized by the deposition of beta-amyloid peptide in extracellular neuritic plaques and the formation of intraneuronal neurofibrillary tangles, which elimination has been the unsuccessful goal of different therapies. However, little is known about the progressing neuroinflammatory process, characterized by an increase in the number and morphological changes of microglial cells at different stages of the disease. The aim of this study is to characterize the morphological differences of microglial cells in the hippocampus of an aged murine model of Alzheimer's disease to elucidate whether, associated with age and tau and beta amyloid deposits, there is an active proinflammatory phenotype different from the physiological pattern and how it is related to the formation of tau neurofibrillary tangles.

Twelve female mice (healthy controls and 3xTgAD, n = 6 per group) between 19 and 22 months were used and 10 cells from each animal were randomly analysed using the AnalyzeSkeleton and FracLac extensions of the Image-J program. No significant differences were found between both groups. Secondly, we studied microglial relationship with tau accumulation in controls and 3xTgAD animals at different stages (9, 12 and 15 months, n=3). Our results show an increase in both the number of microglia cells and intracellular tau tangles associated with age, as well as a strong relationship between both variables.

In sum, we must consider the age variable to understand the rol of microglial cells in AD neurodegeneration process. Understanding their morphological heterogeneity may be one of the keys of this neurodegenerative disorder.

Key Words: *Alzheimer's disease, microglia, neuroinflammation, animal model, fractal analysis, tau, β-amyloid.*

1. INTRODUCTION

Dementia is an age-related disease that involves impairment of memory, intellect, behaviour, and the ability to perform activities of daily living (Vatanabe et al., 2019; Hashemiaghdam & Mroczek, 2020). It currently affects about 50 million people and is expected to affect 100 million more by 2050 (Alzheimer's Disease International, 2019). Alzheimer's disease is the most common form of dementia, representing 60-70% of cases (Bello-Medina et al., 2019). At the neuropathological level, this disease is characterized, among others, by the presence of protein deposits of β-amyloid peptide (Aβ) in extracellular neuritic plaques (SP) and the formation of intraneuronal neurofibrillary tangles of tau protein (NFT) (Hardy & Higgins, 1992; Zetterberg & Bendlin, 2021), an exacerbated neuroinflammation (Calsolaro & Edison, 2016; Song, 2018), synaptic loss (Hickman et al., 2018), increased oxidative stress (Bello-Medina et al., 2019; Bartels et al., 2020) and selective neuronal death (Hashemiaghdam & Mroczek, 2020).However, from a macroscopic point of view an AD brain does not differ significantly from one that has undergone physiological aging (Pini et al., 2016). Cortical and subcortical atrophy selectively affecting the hippocampus, accompanied by a predominant dilatation of the temporal horn of the lateral ventricle are postulated as the unequivocally specific, and microscopically-related features of AD (Perl, 2010).

During decades, the hypothesis of the β-amyloid cascade, first described in 1992 by John A. Hardy and Gerald A. Higgins, was the predominant one (Hardy & Higgins, 1992). This theory suggests that it is the accumulation of these proteins that triggers synaptic dysfunction and increased phosphorylation and secretion of tau (Hardy & Higgins, 1992; Zetterberg & Bendlin, 2021). Associated with this hypothesis emerged numerous therapies focused on trying to eliminate the formation of these deposits obtaining unfruitful results (Lue et al., 2019). In parallel to these theories, others emerged that gave more importance to the accumulation of neurofibrillary tangles because of two main aspects: i) the direct correlation, at the beginning of the symptomatology, of NFT number with cognitive impairment, and ii) in addition to AD, tangles were found in more than 20 different neurodegenerative diseases (tauopathies) (Spillantini & Goedert, 2013), and, except for AD, most of these diseases occur without amyloid deposition and many are associated with tau mutations, suggesting that tau dysfunction and/or tangle formation contribute to disease aetiology (Naseri et al., 2019). Even more, it has also been demonstrated that there is no correlation between senile plaques and cognitive impairment (Dickson et al., 1992; Spillantini & Goedert 2013).

Beyond these deposits, the existence of microglial cells that both increase their number and modify their ramifications in response to or associated with neurodegenerative processes has been known since the last century (McGeer et al., 1987). In this sense, a new etiological hypothesis emerges suggesting that excessive production of cytotoxic cytokines, reactive oxygen species or degradation enzymes by microglia may be early events in the pathogenesis of the disease and accelerate the neurodegenerative process (Leng & Edison, 2020). Microglial cells, a specialized population of tissue resident macrophages, are considered immune

sentinels in the central nervous system (CNS), play an essential role in maintaining homeostasis (Li & Barres, 2018; Brioschi et al., 2020), participating in the regulation of brain development (Mosser et al., 2017; Brioschi et al., 2020), maintenance of neural networks (Bohlen et al., 2019), and injury repair (Hickman et al., 2008). Moreover, as a major source of proinflammatory cytokines, are the key mediators of neuroinflammation, modulating a wide spectrum of cellular responses (Yuan et al., 2020).

In a steady state, these cells present a central soma from which project multiple dynamic extensions that are responsible of monitoring their environment (protruding and retracting), and eliminating dying cells, and remodelling synapses through a continuous pruning process (Lara-Ureña, 2020). Defects or dysfunctions in synaptic pruning produce learning abnormalities and cognitive defects (Hickman et al., 2008). The activation states of microglia could be classified, like the rest of macrophages, into "classical" or M1 and "alternative" or M2 (Martinez & Gordon, 2014). In general, an M1 phenotype represents proinflammatory activity, including the production of proinflammatory cytokines, such as tumour necrosis factor (TNF) and interleukin-1β (IL-1β). Microglia in the M2 state exhibit an anti-inflammatory phenotype associated with Il-10 and transforming growth factor-β (TGF-β) expression, related to wound healing (Martinez & Gordon, 2014; Li & Barres, 2018). Laser-induced microlesions stimulate microglia located in the vicinity of the lesion, which direct their prolongations towards the site of damage to form structures capable of scrutinize the injured tissue (Davalos et al., 2005). Major damage or inflammatory stimuli induce morphological changes in microglia from branching to amoeboid morphology (Colonna & Butovsky, 2017), where the cell body enlarges while the branches shorten and cover more limited areas (Colonna & Butovsky, 2017; Lara-Ureña, 2020).

Alzheimer´s disease murine models have evidenced a reduced expression of microglial receptors for Aβ phagocytosis, but maintain their ability to produce proinflammatory cytokines, suggesting that the accumulation of β-amyloid is due to, in part, to a failure in Aβ microglial scavenger function (Hickman et al., 2008). It has also been described how microglia forms a physical barrier to contain SP and protect neurons from neurodegeneration (Condello et al., 2015). The function of microglial cells would resemble the famous two-sided coin of the god Janus, while their early activation is beneficial in removing toxic β-amyloid from the brain, over time, chronic stimulation becomes detrimental and leads to a prolonged neuroinflammation, excessive deposition of Aβ and thus accelerates the neurodegenerative process (Wang & Colonna, 2019). However, although research to date has shown significant morphological differences between control and experimental animals, most of these studies have been carried out in early stages of the pathology, using young and/or male animals, without considering the age and/or gender variable.

In relation to these murine models, and particularly relevant to this work, AD features have been recapitulated in the 3xTg-AD mouse model. This model develops age-dependent Aβ and tau pathologies (Oddo et al., 2003), along with increased microglia and activated astrocytes in response to plaque deposition (Kitazawa et al., 2005), and progressive cognitive impairment

(Billings et al., 2005). This mouse model has been useful in elucidating several pathways by which Aβ accumulation controls tau phosphorylation, suggesting that β-amyloid levels are upstream of tau accumulation (Oddo et al., 2004). Furthermore, it has been shown that aspects of a dysregulated inflammatory response, both in transgenic mouse models of AD (Parachikova & Cotman, 2007) and in AD patients (Parachikova et al., 2007), can lead to cognitive impairment. Therefore, 3xTgAD murine model is extremely appropriated for our two main objectives. Firstly, to characterize the morphological differences of microglial cells in the hippocampus to elucidate whether, associated with age, there is an active proinflammatory phenotype different from the physiological pattern. Secondly, to establish what is the relationship of this neuroinflammatory microglial pattern with the appearance of neurofibrillary tangles at different temporal patterns: 9, 12 and 15 months old.

2. **METHOD**

2.1. Animals

Experiments were performed in 3xTg-AD mice harbouring three human mutant genes: PS1M146V,APPSWE and tau (TauP301L) and in age-matched wildtype (WT) animals (WT: C57BL6/129S background). WT mice used in this study have the same genetic background of the presenilin knockin embryos used to generate the 3xTg-AD mouse model, but instead of expressing mutant PS1M146V gene they express the endogenous WT mouse PS1M146V gene. The animals were maintained at 32 ± 1 ◦C, 60% relative humidity, on a 12 h light– dark cycle, with access to water and food ad libitum. 3xTgAD and wildtype littermates were bred in the SEA animal care facility. The animal experimentation was conducted in accordance with the guidelines established by Spanish legislation (RD 53/2013) and the European Union regulation (2010/63/EU) and also with the European Community directive guidelines for the use of animals in laboratory (2010/63/EU). All the procedures were approved by the Ethics Committee of the Universitat Jaume I (approval number 2015 / VSC / PEA/00213).

A total of 40 female animals (20 control and 20 3xTgAD mice), aged between 19 and 22 months (n=6) or 9, 12 and 15 months (n=3 animals each age) were used. Female mice were chosen not only because they are more susceptible to Alzheimer-type pathology and longer-lived than male mice but also because its scientific interest since most previous studies used male 3xTgAD mice model.

2.2. *Tissue samples processing*

Briefly, animals were anesthetized by intraperitoneal administration of sodium pentobarbital (Dolethal, 200 mg/kg i.p; Vetoquinol S.A., Madrid, Spain), transcardially perfused with 0.9% saline solution (50 ml) and subsequently fixed with paraformaldehyde (4% in 0.1 M PB, ph=7.4) for 12 min (60 ml). Brains were quickly removed, dissected, and cryoprotected for 3 days in 30% sucrose that was dissolved in 0.1 M phosphate buffer.

Sliding Microtome Leica SM2010R (Leica Microsystems, Heidelberg, Germany) was used to obtain 40-µm thick coronal frozen sections that were preserved in cryoprotective solution at -20°C until the day immunohistochemistry was performed.

2.3. Immunohistochemistry

For immunofluorescence, two 40 µm hippocampal sections were selected in each animal. At late stages (19-22 months old) only macrophage and microglia specific calcium-binding protein (Iba1) was performed, while, to study their relationship with tau tangles, (9,12, and 15 months old) double staining was performed to label both Iba-1 and tau deposits. Non- specific Fc binding sites were blocked with 10% normal goat serum, and the sections were incubated for 24 h (room temperature, constant shaking) with primary antibody diluted in PBS containing 1% goat serum, 0.3% Triton X-100. Rabbit Anti-Iba1 (1:1000, Wako Chemicals, United States) and Mouse Anti-human PHF-tau (1:500, Fisher Scientific SL, Rockford, United States) were used. The sections were incubated for 2 h with the labelled secondary antibody and were then washed with PBS and incubated with the DAPI solution (1:1000) in 1× PBS for 1 min. The sections were washed, mounted with Fluorsave mounting medium (Merck Millipore), and examined using either fluorescence or confocal microscopy. The secondary antibodies used are as follows: Alexa 488 goat antirabbit secondary antibody (1:500, Jackson ImmunoResearch, West Grove, PA, United States) and Cy3 goat anti-mouse (1:200, Jackson ImmunoResearch, West Grove, PA, United States).

2.4. *Image acquisition and analysis*

2.4.1. Microglia cell morphology

The brain sections were examined using a TCSSP2 laser confocal scanning coupled to a Leica inverted DMIRB microscope and Leica Confocal Software (Leica Microsystems). Iba-1 detection was associated with Alexa fluorophore 488 that absorb light maximally at 493 nm and fluoresce with a peak around 519 nm and DAPI that absorb light maximally at 405 nm and fluoresce with a peak around 491 nm.

A series of optical sections were analysed to determine an upper and lower threshold using the Z/Y position for the Spatial Image Series setting. The optical series covered a 20 µm thick slice of tissue with 0.4 µm per optical section. The confocal microscope settings were established and maintained by local technicians for optimal resolution. All images were captured using the 40x dry objective. Three images of the CA1 region of the hippocampus were obtained and analysed with Image-J software following the University of Arizona protocol (Young & Morrison, 2018) (download FIJI/ImageJ from https://imagej.net/Fiji/Downloads). Ten cells from each animal were randomly selected and AnalyzeSkeleton (2D/3D) (http://imagej.net/AnalyzeSkeleton) and FracLac (https://imagej.nih.gov/ij/plugins/fraclac/fraclac.html) extensions were used to analyse different parameters of microglial cells. These plugins provide rapid analysis of microglial

branching and morphology. This process is remarkably time consuming but provides very good results with respect to microglial cell complexity, shape, and size.

2.4.1.1. AnalyzeSkeleton plugin

This plugin analyses multiple cells within a region of interest and provides us an image "labelled" with the branch length. Briefly, we separate both channels (DAPI and Alexa 488) (Image-Color-Split Channels) and choose a maxim-intensity z-project that three-dimensionally includes whole cells (Image-Stacks-Z project). Once, we have selected our ten cells, a series of filters must be applied so that the image can be correctly analysed (Young & Morrison, 2018) (figure 1).

i. Image - Adjust - Brightness/Contrast → This is one of the most important steps setting the background as dark as possible.
ii. Process - Filters - Unsharp Mask → Optionally can increases the contrast.
iii. Image - Adjust - Threshold → We convert the image to binary to perform the final analysis.
iv. Process - Noise - Despeckle → Optionally, the image could be "cleaned" of loose branches.
v. Process - Binary – Close → Optionally, loose pixels that may belong to branches of cells of our interested could be recovered.

Finally, we save the obtained image as "binary", format needed to perform the fractal analysis obtain, and analyse the skeleton of the complete image (Analyze - Skeleton - Analyze Skeleton (2D/3D)) (Figure 1).

2.4.1.2. Fractal Analysis plugin

This plugin quantifies the microglia complexity considering endpoints and branch lengths. The program calculates the fractal dimension using a "box plot" protocol that determines the number of pixels with an increasing scale, where N is the number of pixels (Young & Morrison, 2018). Using the binary image, we have previously obtained we select the cells we want to analyse. Using the brush tool, we can erase traces of other cells out of our interest and join branches that have been separated from the rest of the cell with the previous process. Finally, it is necessary to acquire the silhouette to obtain the parameters we are looking for such as the cell's convex hull and bounding circle. Attending to previous literature we analysed the following parameters (Karperien et al., 2013; Morrison et al,. 2017; Fernandez-Arjona et al., 2017; Young & Morrison, 2018; Plescher et al., 2018; Fernandez-Arjona et al., 2019).

A. *Fractal dimension.* It measures the complexity of cellular patterns. Higher values mean greater complexity.

B. *Lacunarity*. It is associated with changes in the soma and its morphological characteristics. Low values indicate homogeneity, with the different parts of an image having similar variation. Conversely, high values imply heterogeneity since the image contains many spaces or "gaps" of different sizes.

C. *Density* (also called *solidity*). It is calculated by dividing the area of the cell by the area of its shape. Higher values mean amoeboid shapes.

D. The *area* of the cell. It is quantified as the total number of pixels present in the filled shape of the image, which is then transformed into square micrometres. Higher values indicate larger branches.

E. *Perimeter*. Measures the number of pixels representing the cell outline. Higher values indicate largest branches.

F. *Shape* (called *Span Ratio*). It is the ratio of the major axis to the minor axis. It is related whit cylindrical shape of the cells. Low values indicate that the complexity of their ramifications and their heterogeneity decrease, and they become more compact.

G. *Circularity*. This parameter varies from 0 (linear polygon) to 1 (perfect circle). Same as density, higher values mean amoeboid shapes.

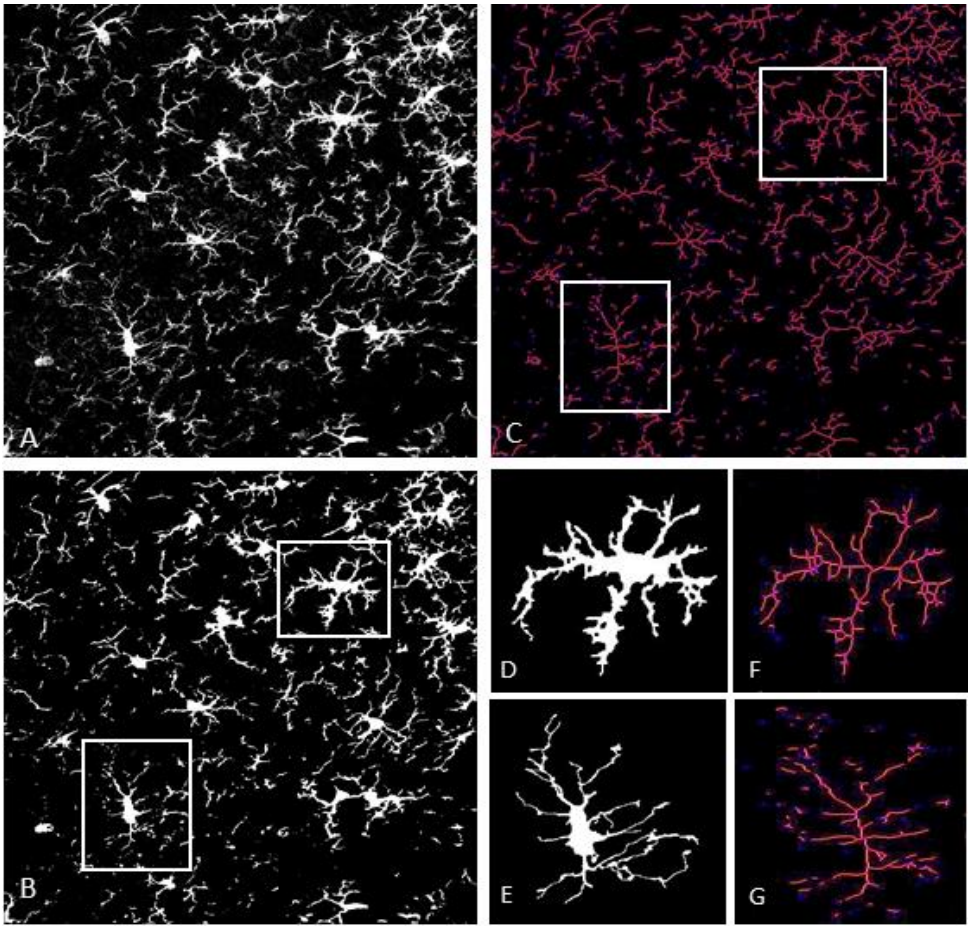

Fig. 1. Example of image processing. (**A**) Original image converted to 8 bits to facilitate the processing. (**B**) different filters are applied to determine more accurately the cell outline (**D** and **E**) Randomly selected cells for fractal analysis. (**C, F** and **G**) skeletonized images from original (**B, D** and **E**) binaries ones, special focus in branch lengths (red) and endpoints (blue).

2.4.2. Relationship between microglia cells and NTF tangle formation

Analysis was performed using an Olympus BX-4CB fluorescence microscope (OLYMPUS CORPORATION) coupled to a Leica DFC 550 camera (Leica Microsystems). Alexa488 and DAPI fluorophores maintained previous absorption and emission wavelengths and Cy3 can be excited maximally at 550 nm, with peak emission at 570 nm. Sequential images covering both anterior and posterior CA1 and CA3 areas were captured at 20× magnification using Leica software (V 2.61). All images were subsequently analysed using Image-J software. Microglial cells were only counted if the whole cell (soma and prolongations) could be identified. Total number of cells was counted, without distinguishing their morphology or activation phase, since this is part of another study. Phosphotau+ cells were only quantified if there was a DAPI counterstain.

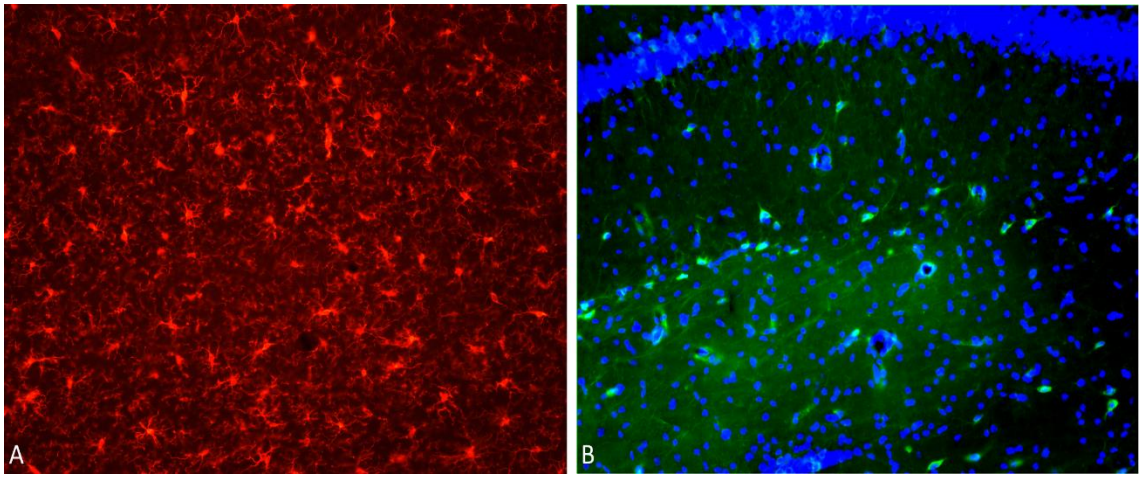

Fig. 2. Photographs of Iba-1 and Phosphotau + cells. (**A**) Image of the IBA1 channel. IBA1+ cells were only counted if the whole cell could be identified. (**B**) DAPI and phosphotau+ cells. Phosphotau+ cells were only quantified when a matching nucleus was present.

2.5. Statistical analysis

The data are expressed as the mean ± SEM and were analysed using GraphPad Prism 9.1.1 (GraphPad Software, San Diego, CA, USA). The normality of the data was assessed with Shapiro–Wilk normality test.

The influence of both variables group (control or 3xTgAD) and age (9,12 and 15 months of age) on the number of microglial cells or NFT (determined by PHF-positivity) was analysed by two-way ANOVA with Tukey's post hoc analysis. The relation between groups was determined by independent t-test analysis.

To establish the relationship between Iba1+ cell number and Tau+ neurons, a simple linear regression and XY correlation analysis were performed, where the independent variable was PHF-positive cells and the dependent variable the number of microglia cells in the control and 3xTgAD groups. Data were considered to be significant at $*p<0.05$, $**p<0.01$ and $***p< 0.001$.

3. RESULTS

3.1. *Morphological changes of microglia cells are dependent on normal aging*.

Research in recent years has related changes in the patterns of morphological and phenotypic parameters of microglia to different pathological conditions, and based on this research, we wanted to evaluate these differences considering the variable age. The morphological and fractal analyses only showed significant differences for the circularity parameter ($p = 0.0072$) (Figure 3B, Table 1). On the other hand, in the rest of the parameters evaluated (fractal dimension, lacunarity, density, area, perimeter and span ratio), no significant differences were found ($p>0.05$) (Figure 3B, Table 1), which indicates that, at these advanced ages, both groups present microglia with an active phenotype (Figure 3A).

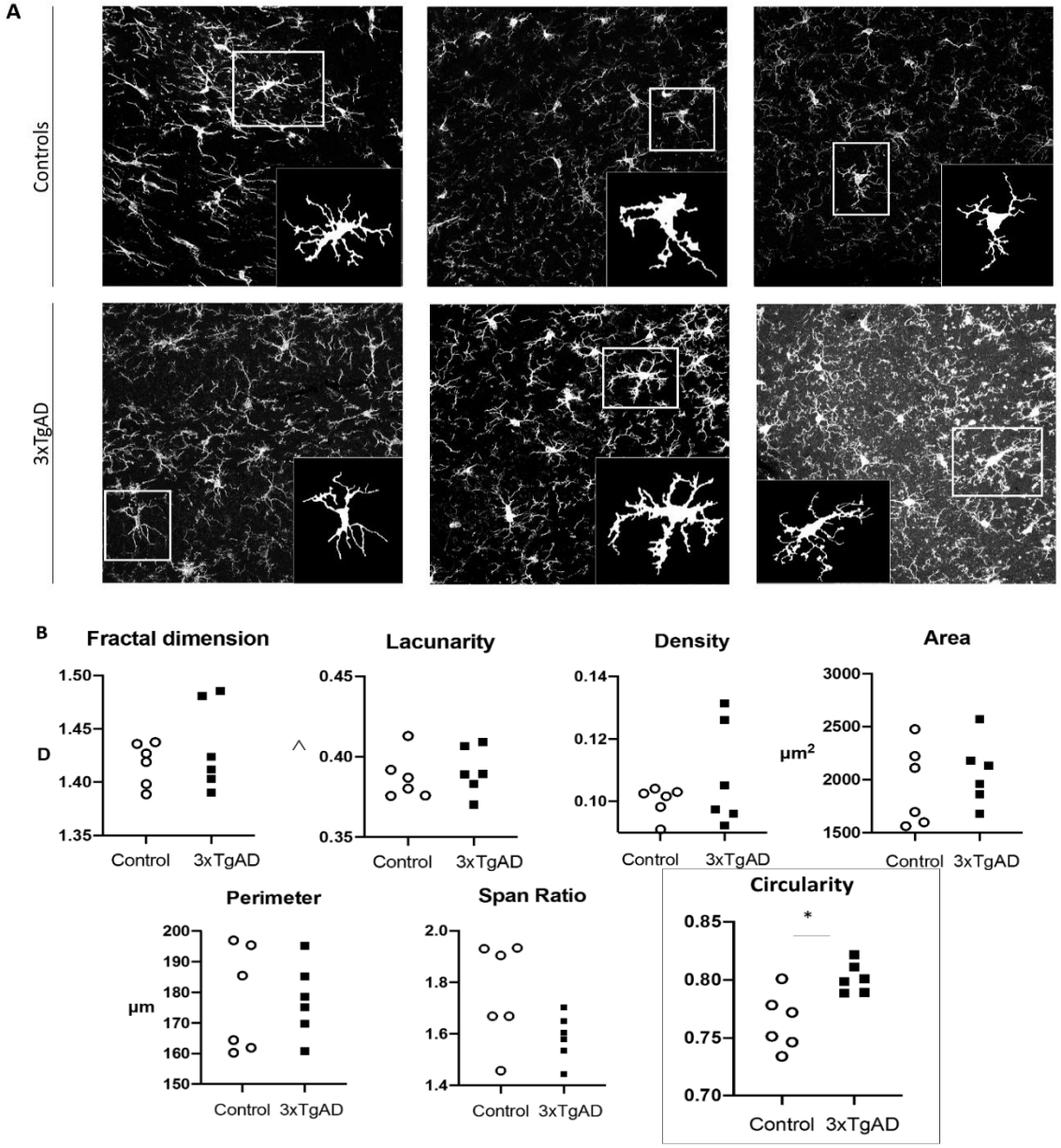

Fig**. 3. Morphological and fractal analysis**. (**A**) Representative processed images from microglia of control and 3xTgAD animals. (**B**) The quantification of the different morphological parameters showed a close morphological similarity between the microglia of both groups (*p<0.05)

Table **1. Quantitative data on microglial morphology.** The means obtained for each of the parameters analysed and the degree of significance obtained are shown. Differences were only observed in the circularity of the microglia, being higher in 3xTgAD animals.

	Fractal D.	*Lacunarity*	*Density*	*Area*	*Perimeter*	*Span Ratio*	*Circularity*
Controls	1.4177	0.3871	0.1000	1945.035	177.4302	1.7602	0.7636
3xTgAD	1.4325	0.3912	0.1080	2064.4845	177.3993	1.5852	0.8016
p	0.44	0.64	0.31	0.56	0.99	0.07	**0.01**

3.2. *The increase in the number of microglia cells is also age-dependent, while the formation of intracellular tau tangles is disease-dependent*.

One of the objectives of our research group is to determine whether the presence of mutations in the APP, presenilin and Tau genes leads to a neuroinflammatory reaction and the formation of deposits and plaques in the hippocampus and whether the presence of plaques correlates with alterations in emotional, social, and cognitive behaviour. The presence of senile plaques (accumulation of beta amyloid) and neurofibrillary tangles (accumulation of tau protein forming "paired helical filaments", PHF) was determined in each temporal space. Previously, we have determined the presence of both accumulations at 9 months of age (Figure 4).

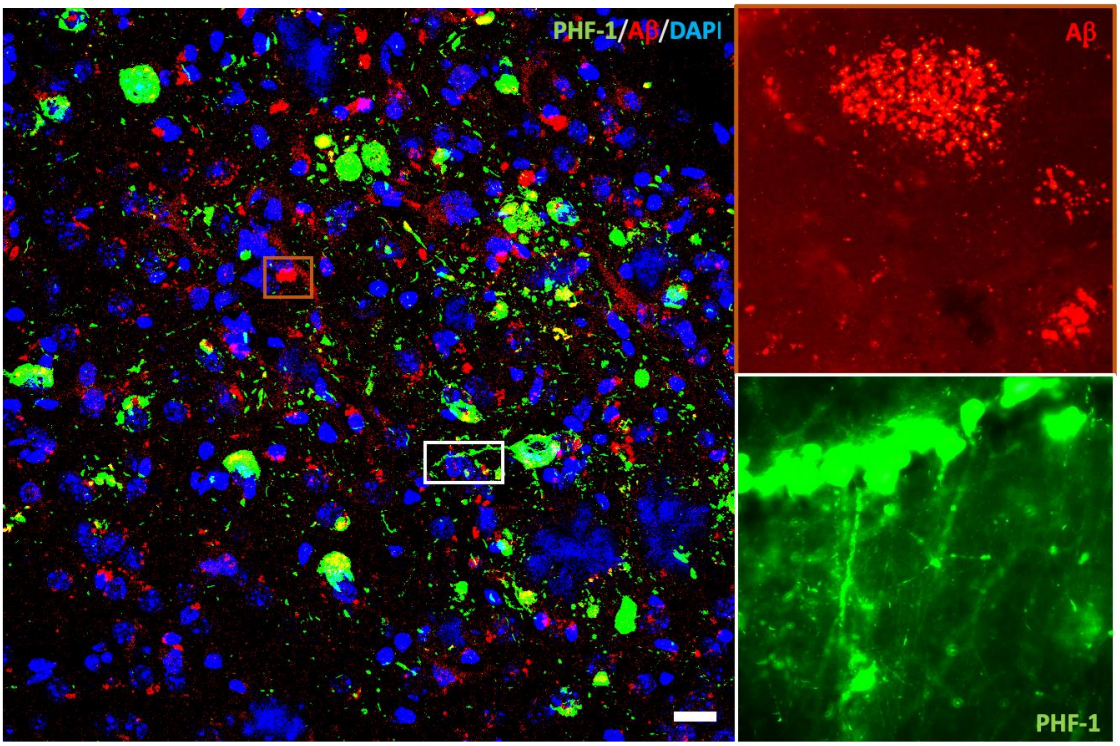

Fig. 4. Presence of neurofibrillary tangles and senile plaques in 9-month-old 3xTgAD mice. The determination of beta-amyloid and tau neurofibrillary tangles was performed with anti-Aβ1-42 and anti-PHF antibody respectively. Scale=20 μm

Since an increase in beta-amyloid and tau accumulation had been observed from 9 months of age we carried out a characterization of the microglial response from that period onwards.

We first determined the number of microglial cells in the CA1 and CA3 regions of the hippocampus of 9-month-old animals. The quantification was also determined at two anatomical levels (ventral and dorsal) (Bregma -2.06 y -29.92 mm). At this age, we observed a significant increase in the number of microglial cells in all regions except the ventral CA3 region (Figures 5 and 8).

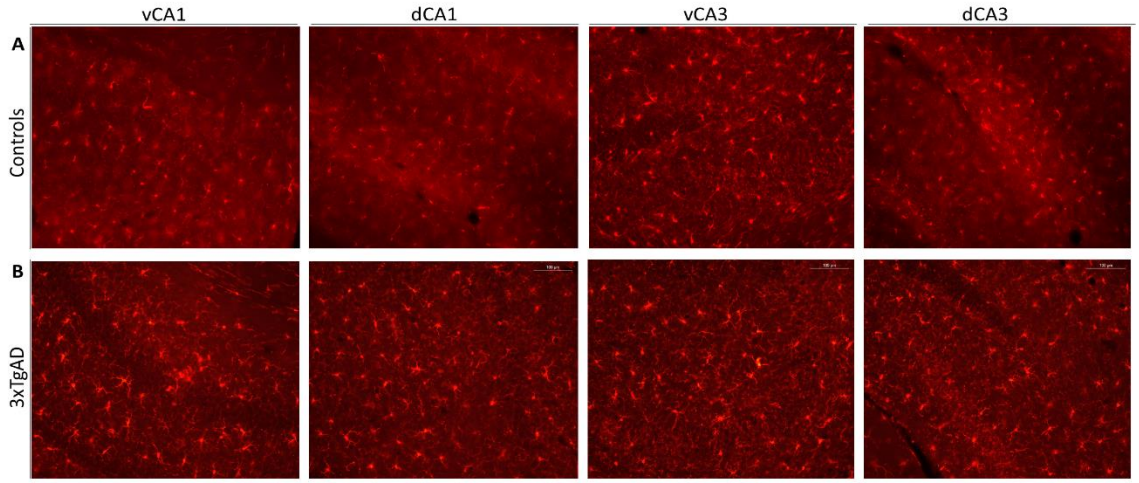

C	*Controls*	*3xTgAD*	*p*
vCA1	83.44	101.10	**0.04**
dCA1	74.53	94.67	**0.002**
vCA3	82.17	83.06	0.68
dCA3	75.50	84.83	**0.04**

vCA1: ventral CA1; dCA1: dorsal CA1; vCA3: ventral CA3; dCA3: dorsal CA3

Fig. 5. Quantification of microglial cells at 9 months of age. Representative images of Iba-1+ cells quantified in hippocampal ventral and dorsal CA1 and CA3 regions of control (**A**) and 3xTgAD (**B**) animals. The means obtained for each group and area and their statistical relationship are shown in the table (**C**). Significant differences (bold) were observed in all the areas analysed but ventral CA3 region (*for further information see figure 8)*.

However, both at 12 and 15 months old, no such massive significant differences ($p>0.05$) between control and 3xTgAD animals could be found (figures 6-8). At both ages, only in ventral CA1 region 3xTgAD showed an increase of microglial cells compared to control animals (figures 6C, 7C and 8). Although the 3xTgAD animals presented an age-associated increase in the number of microglial cells, it was very similar to control animals. This suggest that, as we have previously described with 19-22 months old animals, at late stages the neurodegeneration influence in microglial cells number is made up by the age variable.

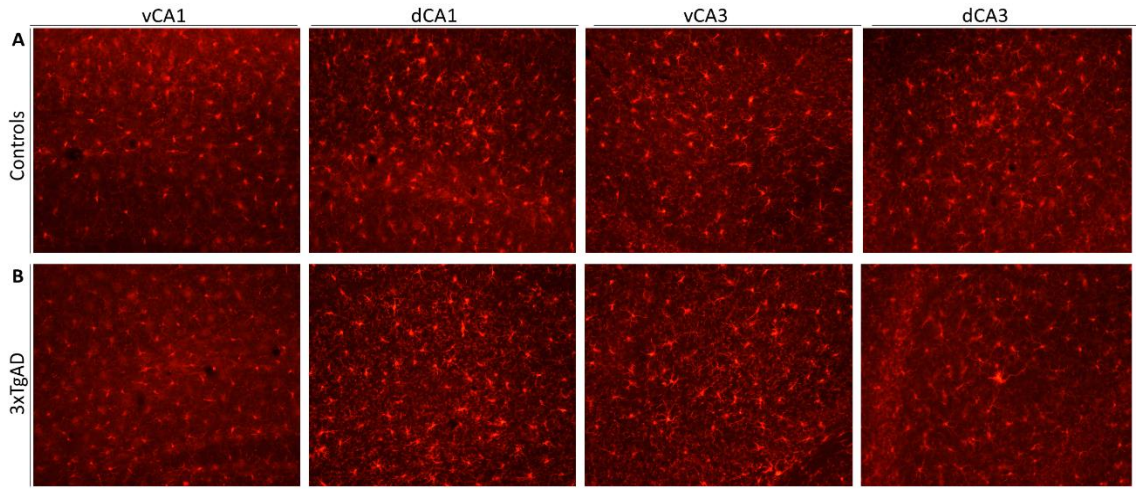

C	*Controls*	*3xTgAD*	*P*
vCA1	98.42	114.50	**0.01**
dCA1	102.60	111.50	0.28
vCA3	100.20	99.83	0.88
dCA3	101.20	101.80	0.9

vCA1: ventral CA1; dCA1: dorsal CA1; vCA3: ventral CA3; dCA3: dorsal CA3

Fig. 6. **Quantification of microglial cells at 12 months of age.** Representative images of Iba-1+ cells quantified in hippocampal ventral and dorsal CA1 and CA3 regions of control (**A**) and 3xTgAD (**B**) animals. The means obtained for each group and area and their statistical relationship are shown in the table (**C**). Significant differences (bold) were only observed in vCA1 area (*for further information see figure 8)*.

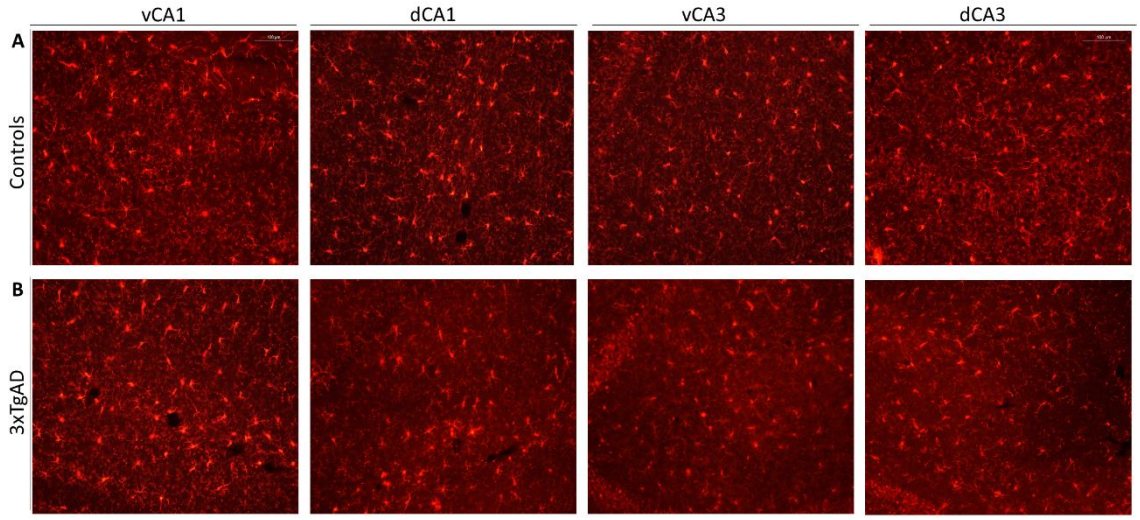

C	*Controls*	*3xTgAD*	*P*
vCA1	107.8	115.7	**0.02**
dCA1	114	110.9	0.57
vCA3	110.8	110.6	0.95
dCA3	106.5	108.9	0.55

vCA1: ventral CA1; dCA1: dorsal CA1; vCA3: ventral CA3; dCA3: dorsal CA3

Fig. 7. **Quantification of microglial cells at 15 months of age.** Representative images of Iba-1+ cells quantified in hippocampal ventral and dorsal CA1 and CA3 regions of control (**A**) and 3xTgAD (**B**) animals. The means obtained for each group and area and their statistical relationship are shown in the table (**C**). Significant differences (bold) were only observed in vCA1 area (*for further information see figure 8)*.

However, the aim of our study was not only to determine whether there were variations in the number of microglial cells at each of the different stages (9, 12 and 15 months of age) but also to determine whether the number of microglial cells associated with age varied in each of these groups (Figure 8).

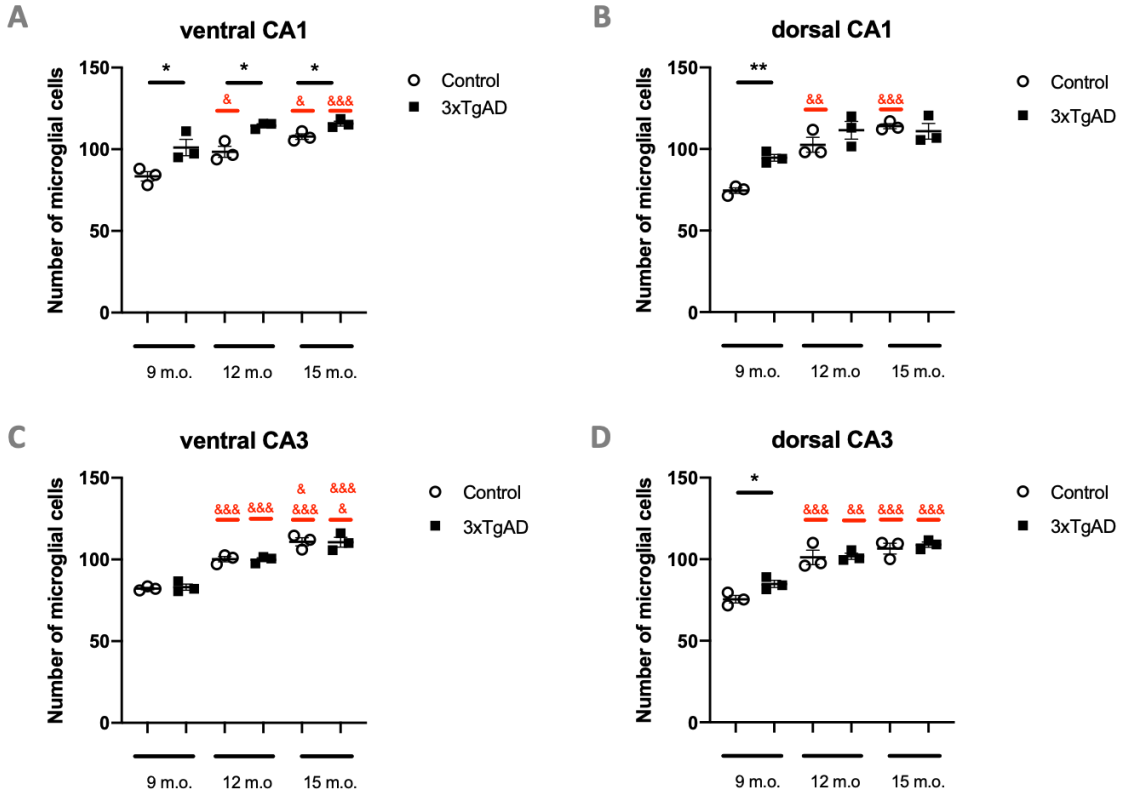

Fig. 8. Effect of the variable age and group on the number of microglial cells in the female 3xTgAD model. The effect of the group (control or 3xTgAD) and time frame (9,12 and 15 months of age) on the number of microglial cells in the areas described above (ventral CA1 (A), dorsal CA1 (B), ventral CA3 (C) and dorsal CA3 (D)) was analysed. Analysis was performed by two-way ANOVA with Tukey's post hoc analysis. Differences intergroup ($^{*}p<0.05$, $^{**}p<0.01$ and $^{***}p< 0.001$) and intragroup ($^{\&}p<0.05$, $^{\&\&}p<0.01$ and $^{\&\&\&}p< 0.001$) are shown.

As can be seen in both the graph and the table, regardless of group, age induces a significant increase in the number of microglial cells, which is most significant between 9 and 12 months in the case of control mice in all areas and in the CA3 region in the case of female 3xTgAD mice (Table 2).

Table 2. Influence of age variable on intragroup number of microglial cells. The significant differences observed for the age variable in each of the areas analysed are shown. The degree of significance of these differences is shown.

	CONTROL			*3xTgAD*		
	9 vs 12 m.o	**9 vs 15 m.o**	**12 vs 15 m.o**	**9 vs 12 m.o**	**9 vs 15 m.o**	**12 vs 15 m.o**
vCA1	$^{\&}p=0.03$	$^{\&\&\&}p=0.0008$	n.s.	n.s.	$^{\&}p=0.04$	n.s.
dCA1	$^{\&\&}p=0.002$	$^{\&\&\&}p<0.0001$	n.s.	n.s.	n.s.	n.s.
vCA3	$^{\&\&\&}p=0.0004$	$^{\&\&\&}p<0.0001$	$^{\&}p=0.02$	$^{\&\&\&}p=0.0007$	$^{\&}p=0.02$	$^{\&\&\&}p<0.0001$
dCA3	$^{\&\&\&}p=0.0003$	$^{\&\&\&}p<0.0001$	n.s.	$^{\&\&}p=0.001$	$^{\&\&\&}p=0.0006$	n.s.

vCA1: ventral CA1; dCA1: dorsal CA1; vCA3: ventral CA3; dCA3: dorsal CA3; m.o: months old; n.s: no significant

Using the Two-way ANOVA we analyzed which variable i) group, ii) age, iii) both or iv) subject determined the variations found in our previous analyses (Table 3).

At hippocampal ventral CA1 level, most of the variations observed were due to both group and age individual variables (35% and 50%, respectively). These results differed from what we found at the dorsal level where, with a percentage next to 70%, the predominant variable was age.

Similar results were observed at both levels of CA3 where the age variable was significantly responsible for the observed changes in percentages that were more than 85% in both cases.

Table 3. Source of variation. Using the Two-way ANOVA test, we determined the main source of variation for each area analysed.

	Group x Age	*Group*	*Age*	*Subject*
vCA1	n.s.	$^{**}p=0.002$	$^{**}p=0.008$	n.s.
dCA1	$^{*}p=0.003$	n.s.	$^{**}p=0.0012$	n.s.
vCA3	n.s.	n.s.	$^{***}p<0.0001$	n.s.
dCA3	n.s.	n.s.	$^{***}p<0.0001$	n.s.

vCA1: ventral CA1; dCA1: dorsal CA1; vCA3: ventral CA3; dCA3: dorsal CA3; n.s: no significant

The other variable we were interested in was tau protein aggregation evidenced by the presence of intraneuronal PHF+ cells in the brain of our female 3xTgAD mice. As expected, significant differences ($p<0.05$) were obtained in all groups in almost all the analysed areas studied. Briefly, we first determined the number of PHF-+ cells in CA1 and CA3 hippocampal regions of 9-month-old animals. The quantification was also determined at two anatomical levels (ventral and dorsal) (Bregma -2.06 y -29.92 mm). At this age, 3xTgAD showed a significant increase in intraneuronal tau deposits in all regions except the dorsal CA3 region (Figure 9).

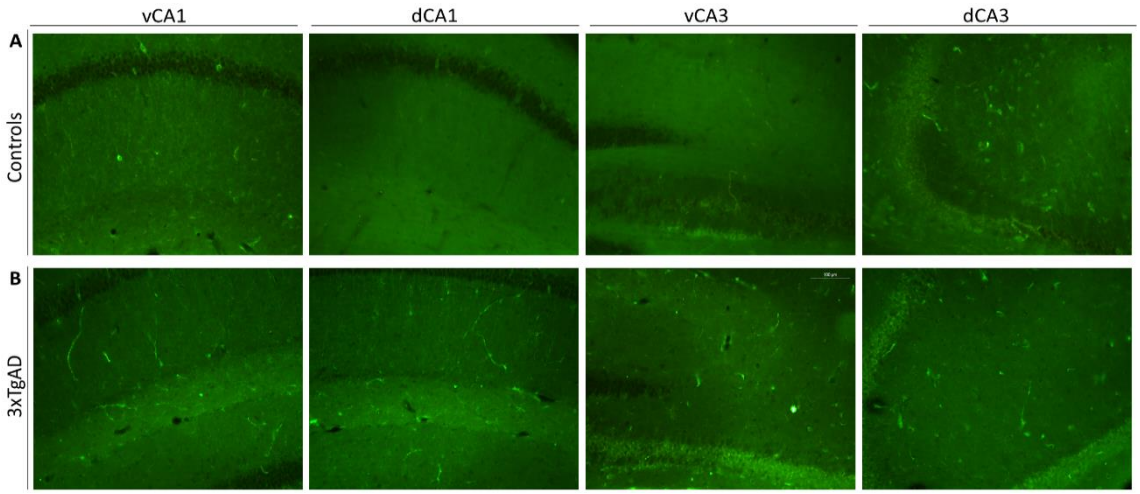

C	*Controls*	*3xTgAD*	*P*
vCA1	20.94	31.08	**0.007**
dCA1	21.61	37.89	**0.02**
vCA3	46.78	60.78	**0.006**
dCA3	48.25	57.67	0.15

vCA1: ventral CA1; dCA1: dorsal CA1; vCA3: ventral CA3; dCA3: dorsal CA3

Fig. 9. **Quantification of PHF-+ cells at 9 months of age.** Representative images of positive cells quantified in hippocampa**l** ventral and dorsal CA1 and CA3 regions of control (**A**) and 3xTgAD (**B**) animals. The means obtained for each group and area and their statistical relationship are shown in the table (**C**). Significant differences (bold) were observed in all the areas analysed but dorsal CA3 region (**C**) (*for further information see figure 12)*.

Analogous results were obtained in control and transgenic animals at 12 months of age. These animals showed a significant increase ($p<0.05$) in the number of PHF-positive cells in our female 3xTgAD animals compared to controls. This increase was present in all areas except in the dorsal region CA3 where both groups had a similar number of PHF-positive cells ($p>0.05$).

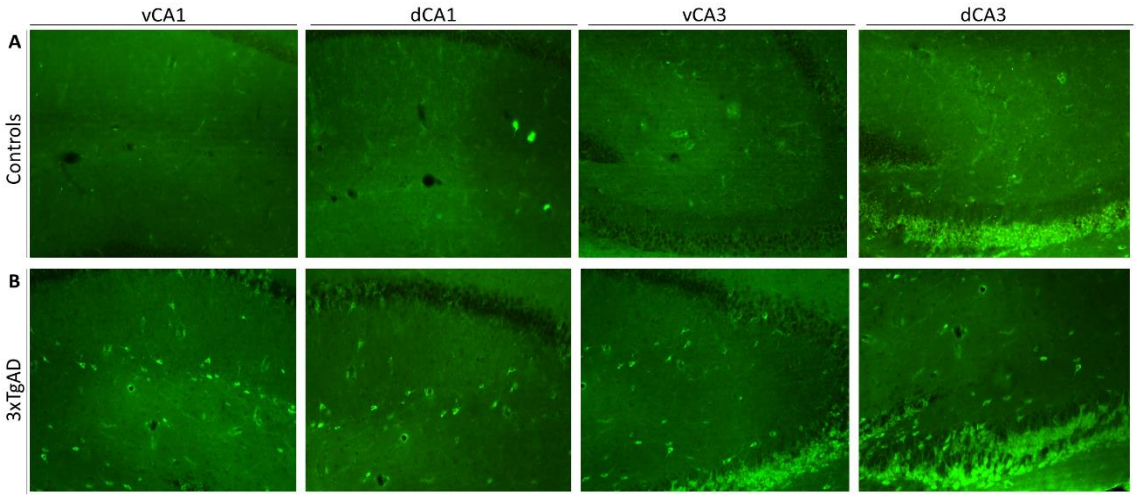

C	*Controls*	*3xTgAD*	*p*
vCA1	35.29	40.95	**0.03**
dCA1	35.22	45.41	**0.03**
vCA3	89.53	97.06	**0.0497**
dCA3	87.64	95.67	0.35

vCA1: ventral CA1; dCA1: dorsal CA1; vCA3: ventral CA3; dCA3: dorsal CA3

Fig. 10. **Quantification of PHF-+ cells at 12 months of age.** Representative images of positive cells quantified in hippocampal ventral and dorsal CA1 and CA3 regions of control (**A**) and 3xTgAD (**B**) animals. The means obtained for each group and area and their statistical relationship are shown in the table (**C**). Significant differences (bold) were observed in all the areas analysed but dorsal CA3 region (**C**) (*for further information see figure 12)*.

In contrast, at 15 months of age, the transgenic animals showed a significant increase in phosphorylated tau deposits in all the areas analysed, being especially significant in the CA3 region.

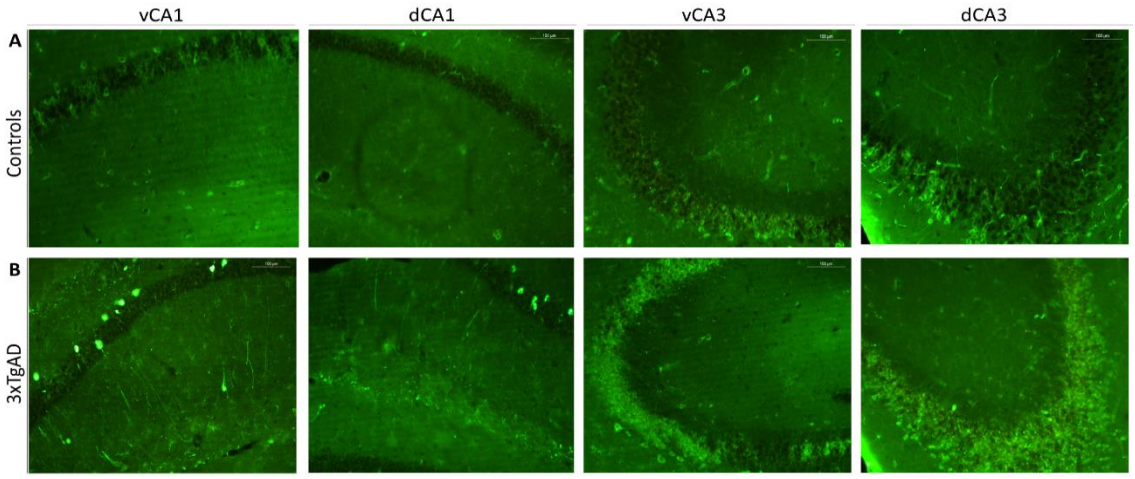

C	*Controls*	*3xTgAD*	*p*
vCA1	43.50	60.43	**0.046**
dCA1	67.92	77.94	**0.02**
vCA3	117.1	166.3	**0.0001**
dCA3	107.2	146.8	**0.004**

vCA1: ventral CA1; dCA1: dorsal CA1; vCA3: ventral CA3; dCA3: dorsal CA3

Fig. 11. **Quantification of PHF-+ cells at 15 months of age.** Representative images of positive cells quantified in hippocampal ventral and dorsal CA1 and CA3 regions of control (**A**) and 3xTgAD (**B**) animals. The means obtained for each group and area and their statistical relationship are shown in the table (**C**). Significant differences (bold) were observed in all the areas analysed (**C**) (*for further information see figure 12)*.

Similar to our study in microglia, we also determined whether, in each of the hippocampal areas analysed, there was an influence of age on the number of PHF-positive cells (Figure 12, Table 4).

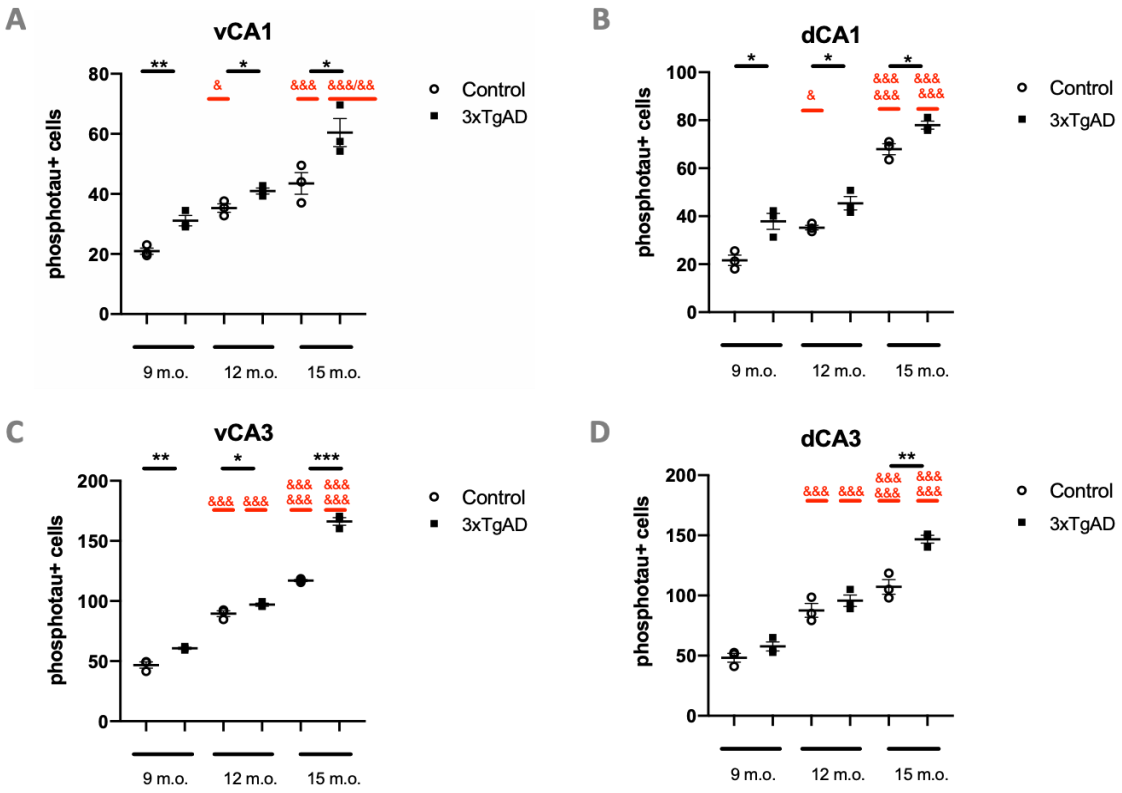

Fig. 12. Effect of the variable age and group on the number of phosphotau-positive cells in the female 3xTgAD model. The effect of the group (control or 3xTgAD) and time frame (9,12 and 15 months of age) on the number of phosphotau (AT8) cells in the areas described above (ventral CA1 (A), dorsal CA1 (B), ventral CA3 (C) and dorsal CA3 (D)) was analysed. Analysis was performed by two-way ANOVA with Tukey's post hoc analysis. Differences intergroup ($^{*}p<0.05$, $^{**}p<0.01$ and $^{***}p< 0.001$) and intragroup ($^{\&}p<0.05$, $^{\&\&}p<0.01$ and $^{\&\&\&}p< 0.001$) are shown.

As can be seen in both the graph and the table, regardless of group, age induces a significant increase in the number of PHF-positive cells, which is most significant between 9 and 12 months in the case of control mice in dCA1 and vCA3 and in the CA3 region. In the rest of areas of control animals there was a significant increase during all the times analysed. On the other hand, 3xTgAD presented a significant increase during the three stages analysed in CA3 area, while the increase in PHF-positive cells were only found between 12 and 15 months old.

Table 4. Influence of age variable on intragroup number of phosphotau-positive cells. The significant differences observed for the age variable in each of the areas analysed are shown. The degree of significance of these differences is shown.

	CONTROL			*3xTgAD*		
	9 vs 12 m.o	**9 vs 15 m.o**	**12 vs 15 m.o**	**9 vs 12 m.o**	**9 vs 15 m.o**	**12 vs 15 m.o**
vCA1	$^{\&}p=0.02$	$^{\&\&\&}p=0.0007$	n.s.	n.s.	$^{\&\&\&}p<0.0001$	$^{\&}p=0.002$
dCA1	$^{\&}p=0.01$	$^{\&\&\&}p<0.0001$	$^{\&\&\&}p<0.0001$	n.s.	$^{\&\&\&}p<0.0001$	$^{\&\&\&}p<0.0001$
vCA3	$^{\&\&\&}p<0.0001$	$^{\&\&\&}p<0.0001$	$^{\&\&\&}p<0.0001$	$^{\&\&\&}p<0.0001$	$^{\&\&\&}p<0.0001$	$^{\&\&\&}p<0.0001$
dCA3	$^{\&\&\&}p=0.0007$	$^{\&\&\&}p<0.0001$	n.s.	$^{\&\&}p=0.001$	$^{\&\&\&}p<0.0001$	$^{\&\&\&}p<0.0001$

vCA1: ventral CA1; dCA1: dorsal CA1; vCA3: ventral CA3; dCA3: dorsal CA3; m.o: months old; n.s: no significant

Using the Two-way ANOVA we analyzed which variable i) group, ii) age, iii) both or iv) subject determined the variations found in our previous analyses (Table 5).

At hippocampal ventral CA1 most of the variations observed were due to the effect of age (almost 70%), similar to what happened at the dorsal level. The same occurred at the dorsal CA1 level as well as in the two levels of CA3, where the age variable was significantly responsible for the observed changes in percentages that were more than 80% in all cases. On the other hand, in contrast to the microglia analysis, individually the group (or disease) variant played a decisive role in the changes observed at the CA1 level. The group variable also induced the changes observed at the CA3 level both individually and age-associated.

Table 5. Source of variation. Using the Two-way ANOVA test, we determined the main source of variation for each area analysed

	Group x Age	*Group*	*Age*	*Subject*
vCA1	n.s.	**p=0.002	**p=0.0015	n.s.
dCA1	n.s.	**p=0.008	***p<0.0001	n.s.
vCA3	***p<0.0001	***p<0.0001	***p<0.0001	n.s.
dCA3	**p=0.003	*p=0.02	***p<0.0001	n.s.

vCA1: ventral CA1; dCA1: dorsal CA1; vCA3: ventral CA3; dCA3: dorsal CA3; n.s: no significant

3.3. *There is a clear relationship between neuroinflammation and pathological tau aggregation*.

Our results show a clear relationship between the increase in the number of microglia cells and the increase in NTF tangles, labelled by PHF-positive cells, in all the groups studied and in all the areas studied (figure 12). This relationship was stronger in the control group animals than in the 3xTgAD animals (0.95 vs. 0.40 anterior part of CA1; 0.76 vs. 0.24 posterior part of CA1; 0.56 vs. 0.24 anterior part of CA3; 0.45 vs. 0.24 posterior part of CA3), which leads us to believe that, under normal conditions, where there are no other variables to contend with (β-amyloid, for example), the relationship increases. These data support the idea that tau pathology in the hippocampus is related to neuroinflammation, in addition to which a loss in microglial surveillance functions may be as or more important than a gain in toxic function in the pathophysiology of AD.

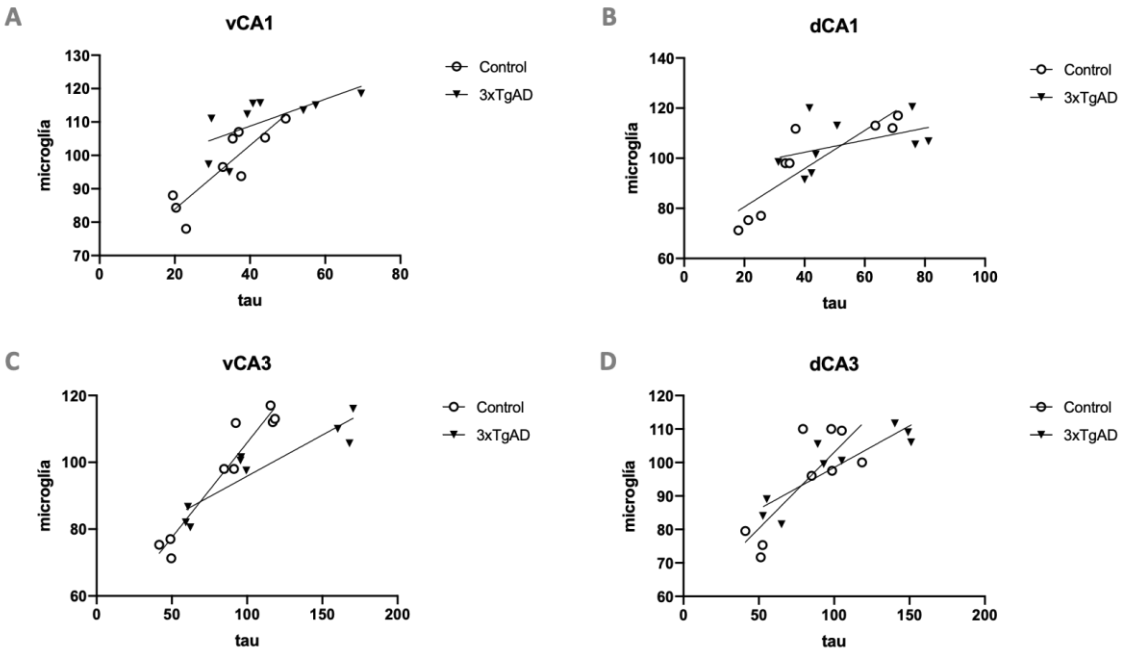

Fig. 13. **Relationship between the number of microglia cells with the number of phospho-tau+ cells.** Slopes: (**A**) ventral part of CA1, 0.95 control group vs. 0.40 3xTgAD group; (**B**) dorsal part of CA1, 0.76 control group vs. 0.24 3xTgAD group; (**C**) ventral part of CA3, 0.56 control group vs. 0.24 3xTgAD group; (**D**) dorsal part of CA3, 0.45 control group vs. 0.24 3xTgAD group.

4. DISCUSSION

The present work is fundamentally novel in two respects. On the one hand, because the entire study was performed in 3xTgAD females, as opposed to most studies to date that address AD models using male mice. On the other hand, because the microglial characterization study was performed at late stages (19-22 months of the disease), so that we have considered the age variable, often ignored in murine models. This age range, 19-22 months will be equal to 65-75 years old in humans (Dutta & Sengupta, 2016).

So, our aims were, on the one hand, to characterize the morphology of microglial cells located in the hippocampus of an aged model of AD. On the other hand, to study the relationship of these cells with the pathological aggregates of tau protein characteristic of the disease at different stages of its development, since it has been studied mainly in relation to Aβ, but, on the contrary, little is known about the inflammatory processes associated with tau pathology.

In relation to the morphology of microglial cells, one of the most comprehensive studies using these software tools, is the analyses of the changes that occur in the neuroinflammation process after injection of the enzyme neuraminidase (NA) at different times (2, 4 and 12h after injection) (Fernandez-Arjona et al., 2017). Arjona and cols. found significant differences in fractal dimension, lacunarity, area, density, and perimeter. This study demonstrated that cellular morphological changes could occur during neuroinflammation process, but they do not

consider either the sex or the age of the animals, which are two variables closely linked to AD and the neurodegeneration process. Furthermore, it is likely that the type of lesion and its temporal and spatial evolution may drive the selective activation of these cells. For example, Zanier et al. demonstrated how microglia with active morphology show a different distribution in three different models of brain injury 24h after injury, and that microglia in brains at advanced stages of disease have more severe morphological changes than those in brains at earlier stages. The descriptors that would best represent the branching of these cells are area and perimeter, while circularity and solidity would provide information about amoeboid shape, that would be related to their function (Zanier et al., 2015). Even so, we must keep in mind the limitations of this morphological study, mainly referred to the use of a two-dimensional approach when analysing three-dimensional cells.

On the other hand, it should be noted that most of the morphological changes found in previous studies are associated with changes in cell density. However, they mostly calculate this parameter as the number of cells divided by the total area of the image. This method is not the most accurate, since, within the same image, microglia can present different morphologies. For example, it has been described how microglia associated with β-amyloid plaques undergo dramatic morphological and electrophysiological changes, while microglia distant to plaques show minor changes (Plescher et al., 2018). Although previous studies have contributed to create a classification of different morphological microglial types, but do not help to clarify when the change occurs, which is one of the most important questions in the pathological study of neurodegenerative diseases. In short, urge to unify a common protocol to increase its reliability and the protocol used in this study and designed by Fernandez-Aroja and cols., could be a good option to alleviate this deficit.

CNS immune cells, such as microglia, appear to be very heterogeneous, with diverse functional phenotypes ranging from proinflammatory M1 phenotypes to immunosuppressive M2 phenotypes, and, although these M1 and M2 have been useful for conceptualizing the activities of microglia in vitro, it is increasingly accepted that this paradigm is not sufficient to describe their activation in vivo, as it rarely shows a significant bias toward one phenotype or another. For example, in models of neurodegeneration, microglia express neurotoxic and neuroprotective factors, genes involved in oxidative phosphorylation, and lysosome, ribosome and spliceosome factors, complexes formed by proteins and RNA that catalyse the production of mature mRNA, involved in responses to misfolded proteins, stress and neuronal death or injury (Colonna & Butovsky, 2017). In this regard, there is a need for further definition of the multiple microglia phenotypes associated with aging, in different neuropathological conditions and at different disease stages. Moreover, recent transcriptomic studies of microglia comparing healthy mice and mice accumulating β-amyloid have identified subpopulations defined as "Disease-associated microglia" (DAM), which are found around plaques, have dysregulated expression of host sensing, maintenance, and defense genes, and appear under conditions of accumulation of neuronal apoptotic bodies and myelin debris (Keren-Shaul et al., 2017; Hickman et al., 2018; Deczkowska et al., 2018). These findings support a direct link

between aberrant microglial functions and AD, and suggest that a subset of microglia switches from homeostatic to DAM in AD.

Previous studies in humans have shown that aged microglia have a different phenotype from activated microglia, showing a dystrophic appearance, represented by a larger soma volume, abnormalities in cytoplasmic structure, retracted and fragmented processes, and a non-uniform tissue distribution. In rodents, results on age-related changes in microglia activation are inconsistent (Edler et al., 2021). In addition, degeneration of microglia cells has also been described in the later stages of human disease, a feature that in animal models is struggling to be found and seems more linked to tau pathology (Sánchez-Mejías et al., 2016). In this work, we have analysed the possible morphological differences existing between healthy late-stage animals and animals from the triple transgenic model of AD. Our initial hypothesis was that the 3xTgAD animals would show more morphological differences in their microglial cells than controls. However, detailed analysis of the different morphological parameters determined that, except for circularity, the two microglial morphologies did not differ. The absence of significant differences highlights the importance of the age variable in understanding the correct functioning of these cell groups in the process of neurodegeneration.

Finally, as we had already commented at the beginning of this discussion, the microglial response has been studied mainly in relation to β-amyloid pathology (e.g., in APP or APP/PS1 transgenic mice, which present a clear and strong microglial activation) and in areas of AD brains with a relatively high β-amyloid content (frontal cortex, for example) (Hayes et al., 2002; Sánchez-Mejías et al., 2016; Serrano-Pozo et al., 2016).

However, of brain regions of relevance in AD development, such as the hippocampus, which have low β-amyloid accumulation and a high number of phospho-tau-bearing neurons, little is known about the inflammatory processes associated with tau pathology (Braak & Del Tredici, 2015; Romero-Molina et al., 2018). Our group has obtained behavioural results (De Castro Salazar, under review) that indicate that in 3xTgAD animals there are differences in social memory that are evident after 9 months of age. One of the main structures involved in social memory is the hippocampus, both at CA1 and CA3 levels. Phosphorylated tau deposits increased significantly in all areas studied between 9-15 months, with the least affected area being the dorsal part of CA3, which, compared to controls, begins to accumulate a greater number of tangles after 15 months. Paradoxically, the number of microglial cells in 3xTgAD animals only increased significantly compared to controls in the ventral area of CA1 between 9-15 months. In both the dorsal area of CA1 and CA3 this increase is only evident at 9 months. The ventral area of CA3 seems to be less affected. This correlates with previous studies that point to the ventral area CA1 as the area where social memory is encoded (Okuyama et al, 2018).

Our study is to date the first to indicate that in this model of AD neuroinflammation would depend on age, so that in aged animals the age variable would even compensate for the morphological differences between the two groups, as we have previously described. On the

other hand, we have seen that the deposits of neurofibrillary tangles would depend as much on the variable age as on the disease itself. Morevoer, our data support the idea that tau pathology in the hippocampus is related to neuroinflammation, but more work is needed to try to clarify the direction of this relationship. For example, in studies with animal models of AD, activation of microglia cells results in tau accumulation and promotes its hyperphosphorylation (Yoshiyama et al., 2007; Maphis et al., 2015), so it has been proposed that loss of surveillance and support by microglia cells may make neurons more susceptible to tau-related neurodegeneration (Paasila et al., 2019). What is clear is that neuroinflammation often coincides in time with tau accumulation, and that the former could be caused by very many factors affecting the brain milieu, including tau pathology itself.

Although our results have an ideal robustness, one of the main limitations of our study is the small sample size used to quantify both microglial cells and phosphorylated tau deposits. We have continued with the analysis the rest of the animals and we hope that these new data will corroborate the results obtained.

In short, the understanding of cell biology has increased exponentially in recent years. Gene expression profiles of microglia are being defined and correlated with specific functions, allowing us to understand the roles of these cells in neurodegeneration and to explore the pathways that regulate their response to injury. But nevertheless, the role of microglia in the pathophysiology of AD remains one of the most critical questions that needs to be answered. Understanding their morphological, transcriptional, and spatial heterogeneity may be the key to uncovering their role in the pathogenesis of neurodegeneration. In the absence of a standardized protocol, we propose Image-J, with its extensions for fractal analysis, as a tool to study the morphology of microglia cells; because it is extremely sensitive to branching patterns and contours, because it has proven effective in analysing microglia, and because the software is freely available to anyone. The model must continue growing, also considering the many, many limitations of this work, like the small number of experimental subjects in each group (for both experiments) and the lack of time to take into account another variables, such as, for example, the relationship with pathological aggregates of β-amyloid too. This is the starting point, and we must be attentive to the possibility that multiple factors affect the morphology of these cells, as well as their function.

5. REFERENCES

Alzheimer's Disease International. (2019). World Alzheimer Report 2019: Attitudes to dementia. London: Alzheimer's Disease International.

Bartels, T., De Schepper, S. and Hong, S. (2020). Microglia modulate neurodegeneration in Alzheimer's and Parkinson's diseases. *Science*, 370 (6512), 66-69. https://doi.org/10.1126/science.abb8587

Bello-Medina, P. C., González-Franco, D. A., Vargas-Rodríguez, I. and Díaz-Cintra, S. (2019). Oxidative stress, the immune response, synaptic plasticity, and cognition in transgenic models of Alzheimer disease. *Neurología,* 2019. https://doi.org/10.1016/j.nrl.2019.06.002

Billings, L. M., Oddo S., Green, K. N., McGaugh, J. L. and LaFerla, F. M. (2005). Intraneuronal Abeta causes the onset of early Alzheimer's disease-related cognitive deficits in transgenic mice. *Neuron*, 45(5), 675–688. https://doi.org/10.1016/j.neuron.2005.01.040

Bohlen, C. J., Friedman, B. A., Dejanovic, B. and Sheng, M. (2019). Microglia in brain development, homeostasis, and neurodegeneration. *Annual Review of Genetics*, 53, 263–288. https://doi.org/10.1146/annurev-genet-112618-043515

Braak, H. and Del Tredici, K. (2015). The preclinical phase of the pathological process underlying sporadic Alzheimer's disease. *Brain,* 138, 2814–2833. https://doi.org/10.1093/brain/awv236

Brioschi, S., Zhou, Y. and Colonna, M. (2020). Brain macrophages in development, homeostasis and disease. *Physiology & Behavior*, 176(1), 100–106. https://doi.org/10.4049/jimmunol.1900821

Calsolaro, V. and Edison, P. (2016). Neuroinflammation in Alzheimer's disease: Current evidence and future directions. *Alzheimer's and Dementia*, 12(6), 719–732. https://doi.org/10.1016/j.jalz.2016.02.010

Colonna, M. and Butovsky, O. (2017). Microglia function in the Central Nervous System during health and neurodegeneration. *Annual Review of Immunology*, 35, 441–468. https://doi.org/10.1146/annurev-immunol-051116-052358

Condello, C., Yuan, P., Schain, A. and Grutzendler J. (2015). Microglia constitute a barrier that prevents neurotoxic protofibrillar Aβ42 hotspots around plaques. *Nature Communications*, 6, 1–14. https://doi.org/10.1038/ncomms7176

Davalos, D., Grutzendler, J., Yang, G., Kim, J. V., Zuo, Y., Jung, S., Littman, D. R., Dustin, M. L. and Gan, W. B. (2005). ATP mediates rapid microglial response to local brain injury in vivo. *Nature Neuroscience,* 8(6), 752-758. https://doi.org/10.1038/nn1472

Deczkowska, A, Keren-Shaul, H., Weiner, A., Colonna, M., Schwartz, M. and Amit, I. (2018). Disease-Associated Microglia: A universal immune sensor of neurodegeneration. *Cell*, 173, 1073-1081. https://doi.org/10.1016/j.cell.2018.05.003

Dickson, D. W., Crystal, H. A., Mattiace, L. A., Masur, D. M., Blau, A. D., Davies, P., Yen, S. H. and Aronson, M. K. (1992). Identification of normal and pathological aging in prospectively studied nondemented elderly humans. *Neurobiology of Aging,* 13 (1), 179-189. https://doi.org/10.1016/0197-4580(92)90027-u.

Dutta, S. and Sengupta, P. (2016). Men and mice: Relating their ages. *Life Sciences,* 152 (1), 244-248. https://doi.org/10.1016/j.lfs.2015.10.025

Edler, M. K., Mhatre-Winters, I. and Richardson, J. R. (2021). Microglia in aging and Alzheimer's disease: A comparative species review. *Cells*, 10(5),1138. https://doi.org/10.3390/cells10051138

Fernandez-Arjona, M. M., Grondona, J. M., Granados-Durán, P., Fernández-Llebrez, P. and López-Ávalos, D. (2017). Microglia morphological categorization in a rat model of neuroinflammation by hierarchical cluster and principal components analysis. *Frontiers in Cellular Neuroscience,* 11, 235. https://doi.org/10.3389/fncel.2017.00235

Fernadez-Arjona, M. M., Grondona, J. M., Fernández-Llebrez, P. and López-Ávalos, M. D. (2019). Microglial morphometric parameters correlate with the expression level of IL-1b, and allow identifying different activated morphotypes. *Frontiers in Cellular Neuroscience.* 13,472. https://doi.org/10.3389/fncel.2019.00472

Ginhoux, F., Lim, S., Hoeffel, G., Low, D. and Huber, T. (2013). Origin and differentiation of microglia. *Frontiers in Cellular Neuroscience,* 7,45. https://doi.org/10.3389/fncel.2013.00045

Hashemiaghdam, A., and Mroczek, M. (2020). Microglia heterogeneity and neurodegeneration: The

emerging paradigm of the role of immunity in Alzheimer's disease. *Journal of Neuroimmunology*, 341 (2020) 577185. https://doi.org/10.1016/j.jneuroim.2020.577185

Hardy, J. A. and Higgins, G. A. (1992). Alzheimer's disease: The amyloid cascade hypothesis. *Science*, 256(5054), 184–185. https://doi.org/10.1126/science.1566067.

Hayes, A., Thaker, U., Iwatsubo, T., Pickering-Brown, S. M. and Mann, D. M. A. (2002). Pathological relationships between microglial cell activity and tau and amyloid b protein in patients with Alzheimer's disease. *Neuroscience Letters*, 331 (2002), 171–174. https://doi.org/10.1016/S0304-3940(02)00888-1

Hickman, S. E., Allison, E. K. and El Khoury J. (2008). Microglial dysfunction and defective β-amyloid clearance pathways in aging alzheimer's disease mice. *Journal of Neuroscience*, 28(33), 8354–8360. https://doi.org/10.1523/JNEUROSCI.0616-08.2008

Hickman, S., Izzy, S., Sen, P., Morsett, L. and El Khoury, J. (2018). Microglia in neurodegeneration. *Nature Neuroscience*, 21(10), 1359–1369. https://doi.org/10.1038/s41593-018-0242-x

Karperien, A., Ahammer, H. and Jelinek, H. F. (2013). Quantitating the subtleties of microglial morphology with fractal analysis. *Frontiers in Cellular Neuroscience.* 7, 3. http://dx.doi.org/10.3389/fncel.2013.00003

Keren-Shaul, H., Spinrad, A., Weiner, A., Matcovitch-Natan, O., Dvir-Szternfeld, R., Ulland T. K., David, E., Baruch, K., Lara-Astaiso, D., Toth, B., Itzkovitz, S., Colonna, M., Schwartz, M. and Amit, I. (2017). A unique microglia type associated with restricting development of Alzheimer's disease. *Cell*, 169, 1276-1290. http://dx.doi.org/10.1016/j.cell.2017.05.018

Kitazawa, M., Oddo, S., Yamasaki, T. R., Green, K. N. and LaFerla, F. M. (2005). Lipopolysaccharide-induced inflammation exacerbates tau pathology by a cyclin-dependent kinase 5-mediated pathway in a transgenic model of Alzheimer's disease. *Journal of Neuroscience*, 25(39), 8843–8853. https://doi.org/10.1523/JNEUROSCI.2868-05.2005

Lara-Ureña, N. (2020). Papel de HIF1 y PHD3 en la microglía de la enfermedad de Alzheimer. (Tesis Doctoral Inédita). Universidad de Sevilla, Sevilla. https://idus.us.es/handle/11441/100986

Leng, F. and Edison P. (2020). Neuroinflammation and microglial activation in Alzheimer disease: Where do we go from here?. *Nature Reviews*. *Neurology*, 17(3), 157-172. https://doi.org/10.1038/s41582-020-00435-y

Li, Q. and Barres, B. A. (2018). Microglia and macrophages in brain homeostasis and disease. *Nature Reviews. Immunology*, 18(4), 225–242. https://doi.org/10.1038/nri.2017.125

Lue, L. F., Beach, T. G. and Walker, D. G. (2019). Alzheimer's disease research using human microglia. *Cells*, 8(8), 1–19. https://doi.org/10.3390/cells8080838

Maphis, N., Xu, G., Kokiko-Cochran, O. N., Jiang, S. and Cardona, A. (2015). Reactive microglia drive tau pathology and contribute to the spreading of pathological tau in the brain. *Brain*, 138, 1738-1755. https://doi.org/10.1093/brain/awv081

Martinez, F. O. and Gordon, S., (2014). The M1 and M2 paradigm of macrophage activation: time for reassessment. *F1000Prime Reports,* 6,13. https://doi.org/10.12703/P6-13

McGeer, P. L., Itagaki, S., Tago, H. and McGeer, E. G. (1987). Reactive microglia in patients with senile dementia of the Alzheimer type are positive for the histocompatibility glycoprotein HLA-DR. *Neuroscience Letters*, 79 (1987), 195-200. https://doi.org/10.1016/0304-3940(87)90696-3.

Morrison, H., Young, K., Qureshi, M., Rowe, R. K. and Lifshitz, J. (2017). Quantitative microglia analyses reveal diverse morphologic responses in the rat cortex after diffuse brain injury. *Scientific Reports,* 7, 13211. https://doi.org/10.1038/s41598-017-13581-z

Mosser, C. A., Baptista, S., Arnoux, I., and Audinat, E. (2017). Microglia in CNS development: Shaping the brain for the future. *Progress in Neurobiology*, 149–150(2017), 1–20. https://doi.org/10.1016/j.pneurobio.2017.01.002

Naseri, N. N., Wang, H., Guo, J., Sharma, M. and Luo W. (2019). The complexity of tau in Alzheimer's disease. *Neuroscience Letters*, 705, 183–194. https://doi.org/10.1016/j.neulet.2019.04.022.

Oddo, S., Caccamo, A., Shepherd, J. D., Murphy, M. P., Golde, T. E., Kayed, R., Metherate, R., Mattson, M. P., Akbari, Y. and LaFerla, F. M. (2003). Triple-transgenic model of Alzheimer's disease with plaques and tangles: Intracellular Aβ and synaptic dysfunction. *Neuron*, 39(3), 409–421. https://doi.org/10.1016/S0896-6273(03)00434-3

Oddo, S., Billings, L., Kesslak, J. P., Cribbs, D. H. and LaFerla, F. M. (2004). Aβ immunotherapy leads to clearance of early, but not late, hyperphosphorylated tau aggregates via the proteasome. *Neuron*, 43(3), 321–332. https://doi.org/10.1016/j.neuron.2004.07.003

Okuyama T. (2018). Social memory engram in the hippocampus. *Neuroscience Research*, 129. 17-23. https://doi.org/10.1016/j.neures.2017.05.007

Paasila, P. J., Davies, D. S., Kril, J. J. and Goldsbury, C. (2018). The relationship between the morphological subtypes of microglia and Alzheimer's disease neuropathology. *Brain Pathology*, 29 (2019), 726–740. https://doi.org/10.1111/bpa.12717

Parachikova, A., Agadjanyan, M. G., Cribbs, D. H., Blurton-Jones, M., Perreau, V. M., Rogers, J., Beach, T. G. and Cotman, C. W. (2007). Inflammatory changes parallel the early stages of Alzheimer disease. *Neurobiology of Aging*, 28(12), 1821–1833. https://doi.org/10.1016/j.neurobiolaging.2006.08.014

Parachikova, A. and Cotman, C. W. (2007). Reduced CXCL12/CXCR4 results in impaired learning and is downregulated in a mouse model of Alzheimer disease. *Neurobiology of Disease*, 28(2), 143–153. https://doi.org/10.1016/j.nbd.2007.07.001

Perl, D. P. (2010). Neuropathology of Alzheimer's Disease. *Mount Sinai Journal of Medicine: A Journal of Translational and Personalized Medicine*, 77(1), 32–42. https://doi.org/10.1002/msj.20157

Pini, L., Pievani, M., Bocchetta, M., Altomare, D., Bosco, P., Cavedo, E., Galluzzi, S., Marizzoni, M. and Frisoni, G. B. (2016). Brain atrophy in Alzheimer's disease and aging. *Ageing Research Reviews*, 30, 25–48. https://doi.org/10.1016/j.arr.2016.01.002

Plescher, M., Seifert, G., Hansen, J. N., Bedner, P., Steinhäuser, C. and Halle, A. (2018). Plaque-dependent morphological and electrophysiological heterogeneity of microglia in an Alzheimer's disease mouse model. *Glia*, 66, 1464–1480. http://doi.org/ 10.1002/glia.23318

Romero-Molina, C., Navarro, V., Sánchez-Varo, R., Jiménez, S., Fernández-Valenzuela, J., Sánchez-Mico, M. V., Muñoz-Castro, C., Gutiérrez, A., Vitorica, J. and Vizuete, M. (2018). Distinct microglial responses in two transgenic murine models of tau pathology. *Frontiers in Cellular Neuroscience*, 12,421. https://doi.org/10.3389/fncel.2018.00421

Sanchez-Mejías, E., Navarro, V., Jiménez, S., Sánchez-Mico, M., Sánchez-Varo, R., Núñez-Diaz, C., Trujillo-Estrada, L., Davila, J. C., Vizuete, M., Gutiérrez, A. and Vitorica, J. (2016). Soluble phospho-tau from Alzheimer's disease hippocampus drives microglial degeneration. *Acta Neuropathologica,* 132, 897–916. https://doi.org/10.1007/s00401-016-1630-5

Serrano-Pozo, A., Betensky, R. A., Frosch, M. P. and Hyman, B. T. (2016). Plaque-associated local toxicity increases over the clinical course of Alzheimer disease. *The American Journal of Pathology*, 186 (2), 375-384. http://dx.doi.org/10.1016/j.ajpath.2015.10.010

Song, J. (2018). Animal model of aluminum-induced Alzheimer's disease. *Advances in Experimental Medicine and Biology*, 1091, 113–127. https://doi.org/10.1007/978-981-13-1370-7_7

Spillantini, M. G. and Goedert, M. (2013). Tau pathology and neurodegeneration. *The Lancet. Neurology,* 12 (6), 609-622. https://doi.org/10.1016/S1474-4422(13)70090-5

Vatanabe, I. P., Manzine, P. and Cominetti, M. R. (2019). Historic concepts of dementia and Alzheimer's disease: From ancient times to the present. *Revue Neurologique*, 176(3), 140–147. https://doi.org/10.1016/j.neurol.2019.03.004

Wang, S. and Colonna, M. (2019). Microglia in Alzheimer's disease: A target for immunotherapy. *Journal of Leukocyte Biology*, 106(1), 219–227. https://doi.org/10.1002/JLB.MR0818-319R

Yoshiyama, Y., Higuchi, M., Zhang, B., Huang, S. M., Iwata, N., Saido, T. C., Maeda, J., Suhara, T., Trojanowski, J. Q. and Lee, V. (2007). Synapse loss and microglial activation precede tangles in a P301S Tauopathy mouse model. *Neuron*, 53, 337-351. https://doi.org/10.1016/j.neuron.2007.01.010

Young, K. and Morrison, H. (2018). Quantifying microglia morphology from photomicrographs of immunohistochemistry prepared tissue using image-J. *Journal of Visualized Experiments*, 136, 1–9. https://doi.org/10.3791/57648

Yuan, C., Aierken, A., Xie, Z., Li, N., Zhao, J. and Qing, H. (2020). The age-related microglial transformation in Alzheimer's disease pathogenesis. *Neurobiology of Aging*, 92, 82–91. https://doi.org/10.1016/j.neurobiolaging.2020.03.024

Zanier, E. R., Fumagalli, S., Perego, C., Pischiutta, F. and De Simoni, M. G. (2015). Shape descriptors of the "never resting" microglía in three different acute brain injury models in mice. *Intensive Care Medicine Experimental*, 3, 7. https://doi.org/10.1186/s40635-015-0039-0

Zetterberg, H. and Bendlin, B. B. (2021). Biomarkers for Alzheimer's disease: Preparing for a new era of disease-modifying therapies. *Molecular Psychiatry*, 26(1), 296–308. https://doi.org/10.1038/s41380-020-0721-9